Catalysis Today xxx (2010) xxx–xxx

Contents lists available at ScienceDirect

Catalysis Today

journal homepage: www.elsevier.com/locate/cattod

The targeted synthesis of single site vanadyl species on the surface and in the framework of silicate building block materials

Ming-Yung Lee [a], Jian Jiao [b], Richard Mayes [b], Edward Hagaman [b], Craig E. Barnes [c,*]

[a] Department of Chemical Engineering, University of California at Santa Barbara, Santa Barbara, CA 93106, United States
[b] Chemical Sciences Division, Oak Ridge National Laboratory, PO Box 2008 MS6201, Oak Ridge, TN 37831-6201, United States
[c] Department of Chemistry; University of Tennessee, 552 Buehler Hall, Knoxville, TN 37996-1600, United States

ARTICLE INFO

Article history:
Available online xxx

Keywords:
Vanadyl
Building block
Single site catalysts
Nanostructured solids
Orthovanadate on silica

ABSTRACT

A new synthetic methodology for the targeted preparation of single site, atomically dispersed vanadyl groups in silicate matrices is described. This methodology requires functionalized silicate building blocks $Si_8O_{20}(OSnMe_3)_8$ that become linked together through vanadyl (≡V═O) groups in the matrix. A sequential addition strategy is illustrated which allows the targeting of specific connectivities for the vanadyl group to the silicate building block matrix (i.e. the number of V–O–Si bonds linking the vanadyl unit). Silicate matrices containing exclusively 3-connected ($OV(OSi_{cube})_3$), 2-connected ($OV(OR)(OSi_{cube})_2$) or 1-connected ($OVCl_2(OSi_{cube})$) vanadyl sites are described and characterized via a wide variety spectroscopic and physical techniques (gravimetric analysis, EXAFS, AA and solid state NMR (^{51}V, ^{29}Si, and ^{17}O)). We demonstrate how the combination of gravimetric, solid state NMR (SSNMR) and EXAFS data can be used to uniquely define the vanadyl sites in these matrices. Furthermore, the use of ^{17}O SSNMR (1D and MQMAS) is illustrated as an indirect spectroscopic probe to follow changes in the ligands bound to vanadium atom within the vanadyl groups in these matrices.

1. Introduction

Methods by which homogeneous arrays of metal sites may be constructed on and within extended solid matrices are of great interest in many fields such as electronic solids and heterogeneous catalysis [1,2]. Supported metal based catalysts have shown a wide variety of fundamental and technologically interesting reactivity in solid acid chemistry [3,4], polymerization reactions and oxidation and reduction processes [5]. A key requirement in many such system is that homogeneous arrays of metal sites be constructed on and within extended solid matrices [1]. The most common methods of chemically binding metal species onto metal oxide support involve exposing the surface to a precursor of the desired metal species either in solution (wet impregnation) [6,7] or in the gas phase (CVD) [8–10]. Surface hydroxyl groups are the most obvious points of attachment for metal cations through simple metathesis reactions [11]. The high densities of this group on typical untreated metal oxide powders frequently requires some tailoring of these binding sites before reaction [12]. Thermal protocols are commonly used to remove potential interferences of physisorbed water as well as reduce the number of surface hydroxy groups via dehydration and reconstruction of the surface [13]. In this way supports may be tailored to produce what are believed to be isolated metal catalyst sites on the surface of a metal oxide support.

All strategies which begin with polycrystalline/amorphous powders suffer first from the inability to predict exactly which surface species will result upon cation binding. Second, it is still quite difficult to target a single surface species even when average surface densities might indicate what attachments should result. Clustering of hydroxyl groups on metal oxide surfaces is well known [12] which, upon cation binding will produce multiple surface species that differ from what average measurements would suggest. Finally, the requirement of site isolation usually places rather low limits on site densities to avoid site–site interactions [14] or aggregated sites that exhibit different and frequently unwanted reactivities.

With these challenges in mind, a research program focused on developing new synthetic approaches to constructing what have been referred to as "next generation" catalysts was begun. Such catalysts must, by design, rigorously contain only a single active site. The goal of preparing well defined single site catalysts is not new and should in theory give rise to higher selectivities than systems with multiple sites. The definition of the active site "ensemble" is critical in the context of surface bound species. A metal site bound to the surface of a solid and in contact with a second fluid medium is defined to first order by all the ligands that are directly bound to the metal of which there are generally two types: those that terminate the support phase and hold metal cations in place on the surface

* Corresponding author. Tel.: +1 865 974 3141.
E-mail address: cebarnes@utk.edu (C.E. Barnes).

0920-5861/$ – see front matter © 2010 Elsevier B.V. All rights reserved.
doi:10.1016/j.cattod.2010.06.029

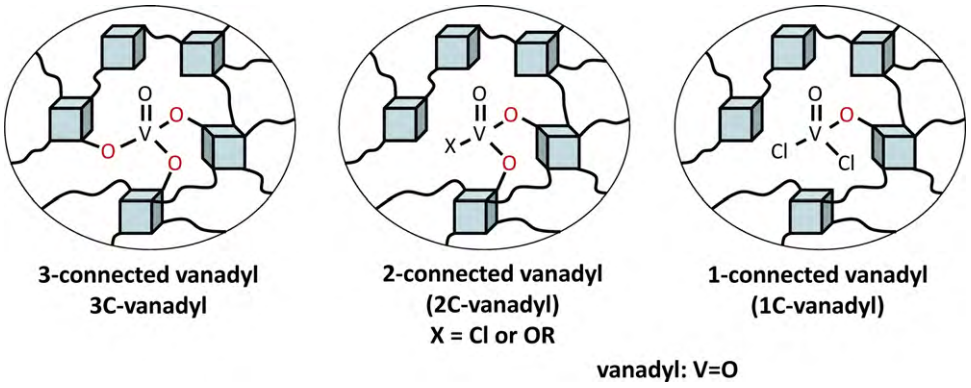

Scheme 1.

and ligands that fill out the rest of the coordination sphere of the ensemble but are not associated with the support. In the past, much attention has been focused on empirical procedures that give rise to a specific number of metal-support bonds in the surface ensemble. However, in most procedures involving a preexisting solid support little control of the spatial geometry of metal-surface bonds can be affected and therefore a distribution of species results even if the desired average connectivity to the surface is achieved. This challenge was approached from a different perspective, namely that the metals which define the active site should participate in each step of the development of the metal-surface interface. The process of creating a surface "imprint" in the immediate environment of the active site should be a critical component of the definition of any single site catalyst [15,16].

Tailored surface binding pockets may also lead to more stable, long lived catalysts in the context of leaching reactions. Overall catalyst activity, however, is dependent on at least two other factors beyond the inherent activity and lifetime of the site itself. Both the number of sites in the system and mass transport processes can also limit activity [17]. Methodologies by which next generation catalysts are prepared should contain well defined strategies by which high site densities are achieved (while ensuring site isolation) as well as high surface areas and mass transport rates.

Two components are required to build such nanostructured matrices: (1) a rigid, nanometer or larger sized molecular building block that will be the main component of the support matrix and (2) two types of chemical linking agents: one that delivers the metal core of the final catalyst ensemble into the matrix and a second that will generate robust chemical linkages between building blocks [18]. With these precursors in hand, a well defined linking reaction must also be identified that involves complementary functionality on the building block and linking agents such that only cross-reaction can occur. Finally, by carefully adjusting both the stoichiometry and sequence of doses of linking reagents and building block, one can target specific connectivities between the building block and metal core of the active site. In this manner, the disposition of the catalyst ensemble can be varied by design from being completely within the framework of cross-linked building blocks to more exposed positions on the surface of a building block support platform.

Atomically dispersed vanadyl groups (VO_4; orthovanadate) on silica have been extensively investigated because of the interesting catalytic behavior exhibited in a number of selective oxidation and polymerization reactions [19–21]. A wide variety of conditions and procedures have been described in the literature to obtain vanadyl groups on support surfaces and much effort has been put into recognizing the distinct spectral signatures exhibited by different surface species that develop as a function of loading and synthetic strategy [22]. It has been reported that loadings between 1–5 wt.% vanadium on silica begin to yield mixtures of isolated orthovanadate centers (VO_4) and VO_x domains containing V–O–V bonds [22–24]. Herein we describe how the combination of building block materials synthesis together with a sequential addition strategy can be used to prepare silicate matrices containing high loadings of atomically dispersed vanadyl groups [25]. Using this strategy, specific connectivities for the orthovanadate groups in these matrices may be targeted (Scheme 1). The synthesis and characterization of isolated 1-, 2- and 3-connected vanadyl centers on the surfaces and in the framework of silica building block solids is described. Finally, an efficient synthetic route for the incorporation of ^{17}O into the bridging oxygen positions around vanadyl groups in these matrices is described. Subsequent ^{17}O SSNMR spectra illustrate how this spectroscopic probe can be used to identify the different types of vanadyl groups present.

2. Materials and methods

2.1. Materials

Experiments with air-sensitive materials were performed under high vacuum or in a nitrogen atmosphere glove box. Diethyl ether, hexanes and toluene were dried over Na/K alloy and distilled. Methylene chloride was dried using calcium hydride and distilled. Vanadylchloride ($VOCl_3$, 99.995%), chlorotrimethylsilane (TMSCl, 98%), and dimethyl–dichlorosilane (Me_2SiCl_2, 99%) were obtained from Aldrich. Tetrachlorosilane ($SiCl_4$ > 99.5%) was obtained from Fisher Scientific. $SiCl_4$, TMSCl, and Me_2SiCl_2 were distilled and stored in Teflon sealed solvent bulbs and capillaries under vacuum. Solvent and reactants were delivered to reaction flasks using vapor transfer methods. Amounts delivered were determined gravimetrically. All glassware was pretreated with TMSCl to remove hydroxyl groups on glass surfaces prior to use.

2.2. NMR spectroscopy

Solution ^1H and ^{13}C nuclear magnetic resonance (NMR) spectra were collect at 7.05 T (Varian Mercury). ^{29}Si solution NMR spectra were acquired at 9.4 T on a Bruker Avance wide-bore multinuclear NMR spectrometer. ^{51}V and ^{29}Si solid state NMR experiments were conducted at 9.4 or 16.4 T, respectively at spin rates of 5–15 kHz on a Varian INOVA 400 and 700 spectrometers. Samples were placed in 5-mm pencil rotors in a nitrogen atmosphere dry box and sealed with paraffin wax. Solid state chemical shifts were referenced externally to ^{29}Si $(Me_3Si)_8Si_8O_{20}$: 11.72 ppm; ^{51}V ($VOCl_3$): 0 ppm. Solid state ^{17}O NMR spectra were acquired on a 16.4T Varian spectrometer at a resonance frequency of 94.9 MHz. The spectrometer is equipped with a Varian console and Varian 3.2 mm MAS probe. Samples were typically spun at 20 kHz. One pulse experiments used

Please cite this article in press as: M.-Y. Lee, et al., The targeted synthesis of single site vanadyl species on the surface and in the framework of silicate building block materials, Catal. Today (2010), doi:10.1016/j.cattod.2010.06.029

a solid 90° pulse (1.1 μs) and a 1 s recycle delay. 3QMAS spectra were acquired using a *z*-filtered pulse sequence, mqmas3qzf2d, with optimized pw1X = 3.3 μs, pw2X = 1.1 μs, and pwXzfsel = 10 μs and recycle delay of 1 s. Chemical shifts are referenced to water: $\delta = 0$ ppm.

2.3. X-ray absorption spectroscopy

All XAS samples were prepared under dry nitrogen in aluminum or polycarbonate sample cells with polypropylene windows sealed with two-sided transparent tape. Data were collected in fluorescence mode at the National Synchrotron Light Source (NSLS) beam line X19A (focused beam) with a 12-channel solid-state Ge detector and beam line X18B (unfocussed beam) with a solid-state passivated implanted planar silicon (PIPS) detector. Tunable, monochromatic light was obtained via a Si (1 1 1) double crystal monochrometer. The monochrometer was detuned 30–50% to suppress higher order harmonics. Samples were mounted at 45° to the beam. Details of the data collection protocol (pre-edge, edge and post-edge regions, energy step size, integration times, calibration routines, etc.) can be found in Supplementary material to this manuscript

Three to six scans were collected for each sample. Data analysis was performed with the IFEFFIT [26] data analysis software suite (Athena & Artemis). The Athena program was used for XANES analysis and extraction of EXAFS from the smooth absorption edge background using standard procedures. Merged files were generated after auto aligning several scans in Athena program. The Artemis program was used for modeling EXAFS $\chi(k)$ data. The theoretical phase and amplitude functions were generated from FEFF [27]. Preliminary fits to structural models were initiated with coordination numbers set to expected values while backscatterer identity (atomic number) was verified and distances were refined. Once these model parameters converged and were stable, coordination numbers were allowed to vary and generally converged to within 20% of expected values based on the connectivity for the sample determined from gravimetric data.

2.4. Surface area and pore size measurements

Surface area determinations (Brunauer–Emmett–Teller (BET) method) were performed using data from a Quanta Chrome Corp. Nova 1000 High Speed Surface Area and Pore Size Analyzer using nitrogen gas adsorption. The adsorption portion of the nitrogen gas adsorption/desorption isotherms was used to calculate the pore size distribution of the samples.

2.5. Synthesis of 3-connected "embedded" vanadyl groups in Si_8O_{20}-based building block (bb) matrices

1.977 g (1.07 mmol) dehydrated $(Me_3SnO)_8Si_8O_{12}$ was loaded in a Schlenk vessel in a glove box and sealed. 20 mL CH_2Cl_2 was then delivered to the reaction vessel followed by 0.182 g (1.05 mmol) $VOCl_3$ via vapor transfer. The reaction proceeded with vigorous stirring at 40 °C for 24 h. Upon completion the solvent and byproduct, Me_3SnCl, were removed by heating (40 °C) under vacuum for at least 12 h. Gravimetric determination of the connectivity of vanadium to the matrix (mmol $ClSnMe_3$/mmol $VOCl_3$) gave 3.1 ± 0.1 connected vanadyl groups. Based on gravimetric data, the theoretical vanadium wt.% for this material is 3.56 with an average molecular formula of $(Me_3Sn)_5Si_8O_{20}(VO)$. Elemental analysis results (AA/AE) for this sample gave rise to a vanadium content of 3.54 wt.%.

After the vanadium was incorporated into Si_8O_{20}-based building block solids, CH_2Cl_2 was again delivered to the Schlenk vessel followed by $SiCl_4$ or Me_2SiCl_2 via vapor transfer for the second dose treatment. The solution was allowed to react at 40 °C for 12–24 h followed by removal of the solvent and Me_3SnCl byproduct under dynamic vacuum. An off-white solid product was obtained which gravimetric analysis indicated contained a small number of residual trimethyltin groups. Residual Me_3Sn groups were removed by treatment with a slight excess (2–3 eq) (per Sn) of TMSCl to the solid product without solvent and heating at 40–60 °C for 6–12 h followed by the removal of volatile byproducts and excess TMSCl.

2.6. Synthesis of 1-connected "surface" vanadyl chloride species on Si_8O_{20}-based bb-matrix

Surface vanadyl species were prepared by reversing the addition sequence described for embedded vanadyl-containing solids. 3.499 g (1.89 mmol) dehydrated $(Me_3SnO)_8Si_8O_{12}$ was added to a Schlenk vessel followed by 20 mL toluene via vapor transfer. After complete dissolution of all solids, silicon tetrachloride (0.683 g; 4.02 mmol; 1 cube: ~2 $SiCl_4$) or 1.043 g (8.08 mmol) dimethyldichlorosilane (1 cube: ~4 Me_2SiCl_2) was vapor transferred into the reaction vessel depending on the type of building block platform desired. The reaction was heated at 80 °C for 48 h. All volatiles were removed under vacuum and the residue heated at 80 °C for 6–8 h until a fine, white powder was obtained. These silicate "platform" matrices contain isolated, unreacted trimethyltin groups. Reaction of these residual tin groups with excess (~5-fold) $VOCl_3$ was carried out at room temperature for 6 h in methylene chloride. A pale purple powder was obtained after unreacted $VOCl_3$ and $ClSnMe_3$ were removed from the reaction residue under vacuum.

2.7. Synthesis of ^{17}O enriched building block, $(Me_3Sn^{17}O)_8Si_8O_{12}$

Fresh 1.6 M methyl lithium in ether (34 mL, 54.4 mmol) was syringed to a Schlenk vessel and frozen under liquid nitrogen. ^{17}O enriched (40 atm%) water (1.00 mL, 55.6 mmol) was then quickly syringed into the Schlenk vessel followed by 20 mL of dry diethyl ether. The reaction to form $Li^{17}OH$ and CH_4 proceeded cleanly to completion over 4 h at 0–20 °C.

10.98 g (55.1 mmol) of Me_3SnCl was then added to the Schlenk vessel and the reaction mixture stirred for another 2 h to obtain a colorless solution with a LiCl precipitate. Calcium hydride (8 g, 190 mmol) was then added to the solution and the Schlenk vessel equipped with a condenser to avoid evaporation of the solvent. Formation of the labeled trimethyltin ether occurred over 3 days at room temperature according to Eq. (1).

$$2\,Me_3Sn^{17}OH + CaH_2 \rightarrow (Me_3Sn)_2{}^{17}O + Ca^{17}O + 2\,H_2 \quad (1)$$

The resulting solution was quickly filtered into another Schlenk vessel followed by addition of 1.334 g (3.14 mmol) $H_8Si_8O_{12}$. Stirring was continued for 4 h during which time the desired product was formed according to Eq. (2).

$$8\,(Me_3Sn)_2{}^{17}O + H_8Si_8O_{12} \rightarrow (Me_3Sn^{17}O)_8Si_8O_{12} + 8\,Me_3SnH \quad (2)$$

The solvent and byproduct Me_3SnH, were removed under vacuum and the remaining white product, $(Me_3Sn^{17}O)_8Si_8O_{12}$, was heated at 60 °C under vacuum for 12 h (5.2 g, yield: 80%). 4.5 g of crystalline product (70% based on water) was obtained from hot hexanes. Potential waters of hydration in the crystal were removed by heating under vacuum at 80 °C before use. The expected enrichment of ^{17}O in the product was verified by HRMS.

2.8. Synthesis of 3C-vanadyl sample using ^{17}O enriched tin cube

A single limiting does of $VOCl_3$ (1V:$(Me_3Sn^{17}O)_8Si_8O_{12}$) was used to cross-link cubes together and obtain only 3C-vanadyl sites

Please cite this article in press as: M.-Y. Lee, et al., The targeted synthesis of single site vanadyl species on the surface and in the framework of silicate building block materials, Catal. Today (2010), doi:10.1016/j.cattod.2010.06.029

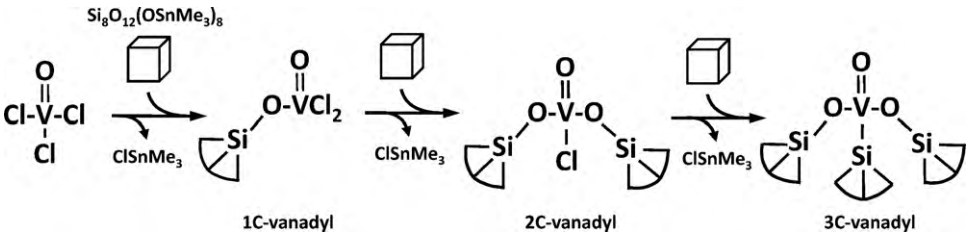

Scheme 2.

in the matrix. The procedure followed was identical to that for unlabeled 3C-materials described earlier.

2.9. Synthesis of "high-V" building block matrix using ^{17}O enriched tin cube

A solution of $VOCl_3$ (10-fold excess per tin) in CH_2Cl_2 under nitrogen was prepared and cooled to −20 °C. Separately, an air free solution of ^{17}O enriched tin cube $Si_8O_{12}(^*OSnMe_3)_8$ in CH_2Cl_2 was prepared in a 30 mL gas tight syringe. The cube solution was slowly syringed into the vanadyl chloride solution over a period of 2 h. The reaction solution turned dark and a precipitate formed. After the addition was complete, the solution was slowly warmed up to room temperature and all volatiles were removed under vacuum, first at room temperature and then at 80 °C overnight. SSNMR MAS analysis of the product indicated that 60% of the corners of the cube were substituted with capping Si–O–$VOCl_2$ groups and 40% were involved in $(\equiv Si–O–)_2VOCl$ groups bridging between two cubes

3. Results and discussion

The strategy described here for constructing single site vanadyl based catalysts in silica matrices rests upon three basic tenets: (1) the availability of suitably functionalized linking reagents and a rigid silicate building block; (2) the ability to cleanly link the two together; and (3) a simple sequential addition strategy by which the specific connectivity of the vanadyl groups between building blocks can be targeted in the final matrix.

The trimethyltin building block ($Si_8O_{12}(OSnMe_3)_8$; "tin cube") and linking reaction used here were first described by Walzer and Feher [28–30]. Trialkyl tin groups on the terminal oxygens of the Si_8O_{20} core cleanly react with the chloride ligands of $VOCl_3$ to produce Si–O–V linkages according to Scheme 2.

All chlorides are found to be reactive such that 2-connected (2C-) and 3-connected (3C-)vanadyl groups readily form in the reaction. To selectively target specific connectivities for the vanadyl groups in the developing matrix, the stoichiometric ratio (V:Si_8O_{20} cube) must be carefully adjusted [18]. Limiting amounts of the $VOCl_3$ should yield oligomeric species containing only 3-connecting vanadyl groups linking three cubes together. Starting with the isopropoxide dichloride complex ($OVCl_2(OiPr)$) and following the same strategy oligomers containing only 2-connecting vanadyl groups are expected. In the context of preparing atomically dispersed vanadyl catalysts on silica-like supports, these mixtures must be further cross-linked together with a reagent that will produce chemically and thermally robust bonds (i.e. not active in catalysis). Silyl chloride reagents are ideal for this purpose and therefore a second round of cross-linking is performed to give the final matrix. The final step in the synthesis of these nanostructured catalysts involves removing all remaining –$SnMe_3$ groups from the

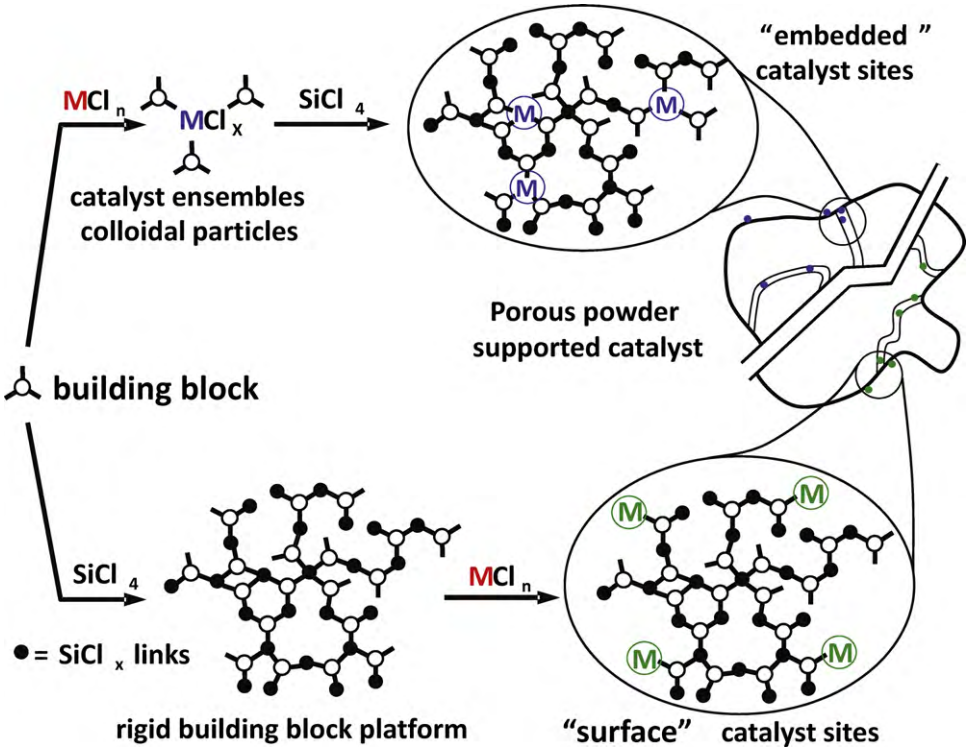

Scheme 3.

Please cite this article in press as: M.-Y. Lee, et al., The targeted synthesis of single site vanadyl species on the surface and in the framework of silicate building block materials, Catal. Today (2010), doi:10.1016/j.cattod.2010.06.029

matrix. Depending on the desired surface properties in the final matrix (hydrophobic vs. hydrophilic) excesses of silyl reagents containing multiple chlorides (e.g. $SiCl_4$) or nonpolar, capping reagents (Me_2SiCl_2, TMSCl) can be used to remove the remaining tin groups.

Matrices in which surface, 1C-vanadyl groups (≡Si–O–$VOCl_2$) are targeted that do not cross-link cubes require an inverse addition sequence. The tin cube is first lightly cross-linked together with one of the above mentioned silyl chloride reagents to produce a silicate building block platform that still contains some unreacted $SnMe_3$ groups. These tin groups will be spatially isolated from one another by virtue of matrix being composed of rigid, 3-dimentionally cross-linked cubes. Final reaction of the platform with $VOCl_3$, regardless of the stoichiometry should produce the desired matrix containing only 1-connected, surface $VOCl_2$ groups. The two arms of this "nanostructuring" strategy that allow us to target and prepare single site catalysts are illustrated in Scheme 3.

In the manner just described, a series of matrices containing atomically dispersed vanadyl groups within the framework and on the surface of cross-linked silicate building blocks have been prepared. Other properties of the matrices that are of interest in the context of catalysis include the following. These matrices are completely amorphous. Under the synthesis conditions (reaction temperatures <80 °C) and assuming cube corners react independently of each other, the formation of cross-links will be both random and irreversible, thus leading to amorphous glasses. We also expect significant void volumes and high surface areas to develop in these matrices. While all of these properties are realized, they are not the primary focus of our present investigations. Surface area data for several of the samples described here are presented in Supplementary material to this manuscript. Strategies to control the growth of these matrices and tailor their meso and macroscopic properties may easily be envisioned and will be described in a future report.

The lines of evidence that are used to verify and characterize the nature of the vanadyl sites in these matrices consist of a combination of simple, well known techniques as well as advanced spectroscopies. The first line is traditional gravimetric analyses of the reaction mixture after each stage of cross-linking. The trimethytin chloride byproduct in the reaction (Eq. (1)) is volatile so that simply removing solvent and Me_3SnCl under vacuum yields an immediate measure of the connectivity achieved by the cross-linking reagent. This well known technique is quick, convenient and at least as accurate as most spectroscopically based techniques for an initial, indirect determination of connectivity.

Table 1
Connectivity versus stoichiometric ratio (V:cube).

V:cube stoichiometry	Achieved connectivity around vanadyl
0.31	3.04
0.65	3.01
0.73	2.95
1.00	3.06
1.23	2.14

The correlation between achieved connectivity and the stoichiometric ratio (V:cube) was investigated briefly and the results are summarized in Table 1. The highest ratio of reactants to cube that can be used and still achieve exclusive 3-connected V=O centers is 1.0. The connectivity drops off at higher ratios presumably due to the increasing size of oligomers that develop and spatial isolation of unreacted trimethyltin groups as more cross-links are formed. In the case when the dichloro vanadyl linking reagent is used, higher stoichiometric ratios may be used and still achieve the limiting 2-connectivity.

Surface bound vanadyl groups have been exhaustively studied by a variety of spectroscopic techniques [8,22,32–38]. X-ray and solid state NMR spectroscopies in particular been used to identify the vanadyl sites in these matrices [8,25,39]. Simple, 1-D ^{51}V NMR spectra can be used to distinguish between 1-, 2-, and 3-connected vanadyl chloride sites in these matrices via empirical correlations between the ^{51}V chemical shift and the number and identify of other substituents bound to vanadium [40–42]. A subset of relevant data from the literature is presented in Table 2. Representative SSNMR spectra for each of the three types of vanadyl sites

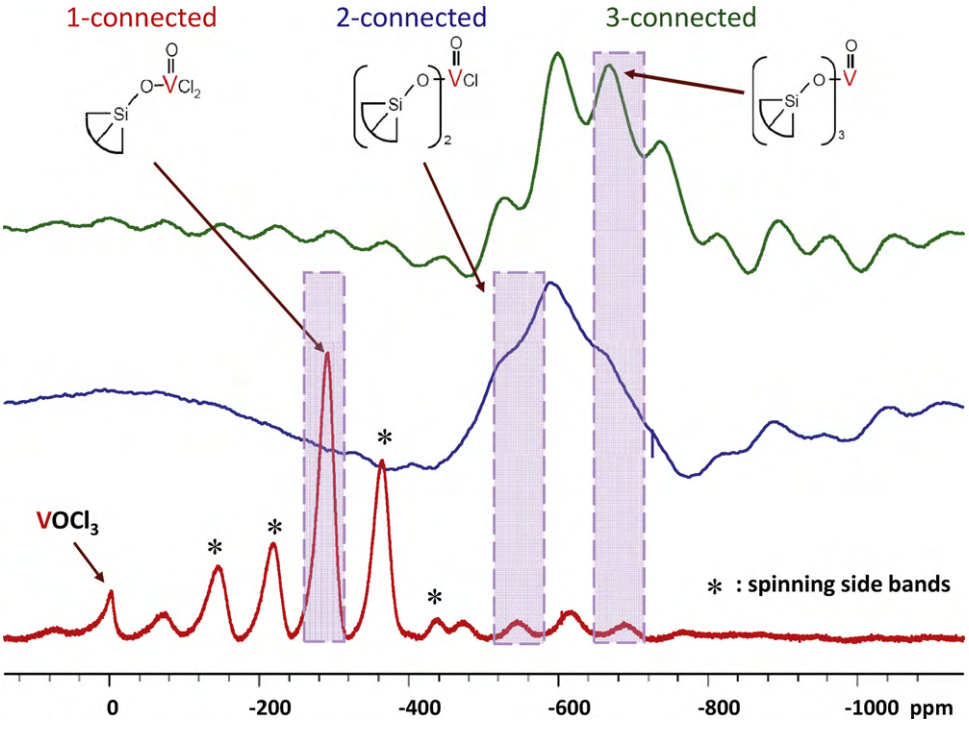

Fig. 1. ^{51}V SSNMR for 1C-, 2C- and 3C-vandyl building block samples.

Please cite this article in press as: M.-Y. Lee, et al., The targeted synthesis of single site vanadyl species on the surface and in the framework of silicate building block materials, Catal. Today (2010), doi:10.1016/j.cattod.2010.06.029

Table 2
^{51}V Isotropic shift SSNMR Data.

Vanadyl complex or surface species	Chemical shift (ppm)	Refs.
$VOCl_3$	0	
$VO(OSiPh_3)_3$	−723	[42]
$VO(OTMS_3)_3$	−711	[31]
$[(c\text{-}C_6H_{11})_7(Si_7O_{12})VO]_2$[a]	−714	[40]
$VO(OSiMe_2)_3$[b]	−736, −727, −705	[31]
∼10% V_2O_5 on SiO_2 (ambient)[c]	−580	[42]
∼10% V_2O_5 on SiO_2 (dehydrated)[c]	−710	[42]
$VOCl(OSi_{silica})(O^tBu)$	−548	[39]
$VO(OSi_{silica})(O^iPr)_2$[d]	−650	[39]
$VOCl_2(OSi_{silica})$[d]	−295	[39,41]
$VOCl_2(OSi_{bb})$ (1C-vanadyl)	−292, −308, −288	This work
$VOCl(OSi_{bb})_2$ (2C-vanadyl)	−545, −540	This work
$VO(OSi_{bb})_3$ (3C-vanadyl)	−680, −692	This work

[a] Dimer of cyclohexyl POSS (polyhedral oligomer silsesquioxane).
[b] Products from reaction of terminating SiOH groups on PDMS with $VO(OAm^t)_3$.
[c] Ambient and dehydrated refer to silica hydrated and calcined silica that was exposed to $VO(O^iPr)_3$ to attach the vanadyl group to the surface.[d]Silica dried at 500 °C before exposure to vanadyl containing complex in the gas phase.

targeted here are presented in Fig. 1 Multiple spectra collected at different spin rates were used to identify the isotropic peak within the envelop of spinning side bands (ssbs) in each spectrum (see Supplementary material, Fig. S1). Although the ssb envelops for the vanadyl sites under study overlap significantly with each other, the spectra show the presence of one predominant envelop around the expected isotropic chemical shift in each case.

The different values for the ^{51}V chemical shifts given in the table for the 1C- and 2C-vanadyl samples represent different stages in the synthesis of these matrices. The first stage is immediately after the first cross-linking reaction of tin cube with a limiting amount of $VOCl_3$. The matrix then contains vanadyl groups and a significant number of trimethyltin groups on unreacted corners of cubes. A second round of cross-linking with either $SiCl_4$ or Me_2SiCl_2 knits the oligomers produced in the first stage into the final, extended building block matrix. Finally, exposure to TMSCl removes residual trimethyltin groups in these matrices. The narrow range of chemical shift values observed for each type of vanadyl group in Table 2 shows that their connectivities do not change during subsequent cross-linking and conditioning steps used to produce final products.

3.1. X-ray absorption spectroscopy

The structural characterization of isolated atomic sites in complex materials is particularly challenging, especially in the case of amorphous solids [43]. X-ray absorption spectroscopy is unique in this context in that it can yield both qualitative and quantitative information about chemical and structural properties of the absorber atom in condensed phases [44]. A typical *K* absorption edge may be divided into three components: (1) features derived from excitation of a 1s electron to virtual states of the absorber atom near the edge; (2) the main absorption edge corresponding to ionization of a 1s electron; and (3) fine structure superimposed on the absorption edge derived from backscattering of the outgoing electron wave by shells of neighboring nuclei around the absorber (EXAFS). Although there have been some attempts to analytically model the first two components above [43,45,46], empirical correlations between pre-edge peak height, width, energy, edge energy and oxidation state and symmetry around the absorber atom are more commonly found in the literature [47]. Likewise, backscattering processes near the edge (XANES) are complex and have only recently begun to be modeled quantitatively [48–50]. Several multiple scattering theories (e.g. FEFF, EXCURVE, GNXAS) are however known for backscattering processes at energies beyond the XANES region (the EXAFS region) that can yield considerable structural information about backscattering shells of atoms around

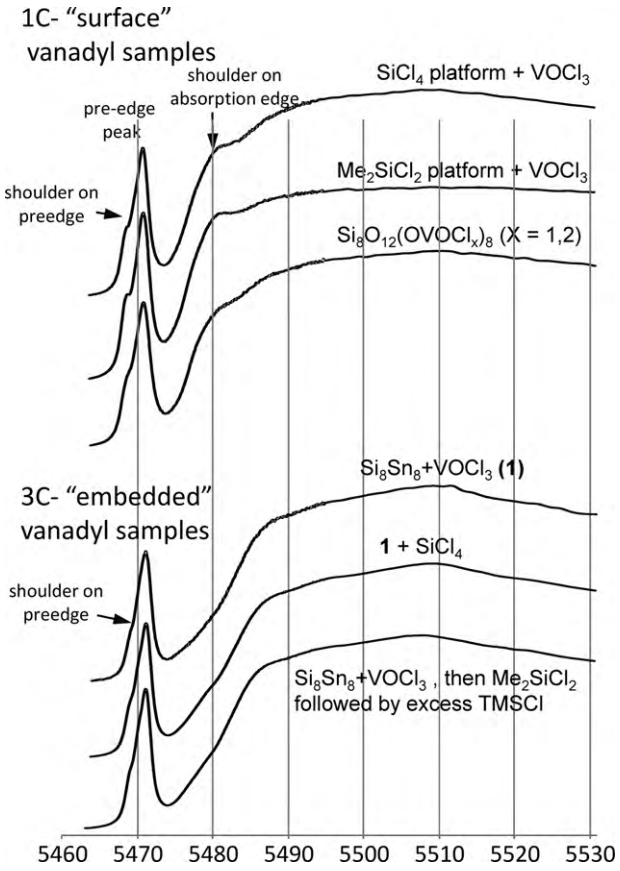

Fig. 2. XANES spectra for 1C- and 3C-vanadyl samples.

the absorber atom [51]. Here we qualitatively analyze the XANES region of the spectra obtained for the different types of vanadyl sites present in these samples as well as develop structural models from EXAFS data.

3.1.1. XANES analysis

Fig. 2 shows overlay plots of the pre- and near-edge regions of the *K*-absorption edge for 1- and 3-connected vanadyl samples. These spectra illustrate the main characteristics seen in all XAS spectra collected in this study. Three main features are observed in this region: a well resolved, intense pre-edge absorption ∼12 eV below the ionization edge; the main ionization edge; and a prominent shoulder superimposed on the ionization edge when chloride is bound to vanadium. The pre-edge absorption peak has been assigned to the 1s → 3d transition [52]. As summarized in Table 3, the position, shape and intensity (peak height) of this pre-edge peak are more or less constant for all the samples studied to date. Table 3 also summarizes two sets of data from the literature that are representative of vanadyl species bound to silica surfaces. s → d transitions for ions in crystal fields with inversion symmetry are first order nonallowed and therefore either not observed or seen as weak absorption peaks in spectra. This selection rule has been qualitatively applied to interpreting the relative intensity of this transition in many previous XAS studies involving vanadium and other transition metals. Generally pre-edge peaks with peak heights >0.7 relative to a normalized edge jump are assigned to coordination geometries without inversion symmetry while those with peak heights <0.7 indicate the presence of sites with O_h symmetry in the sample [8]. O_h symmetry around an absorber ion generally gives rise to multiple low intensity (p.h. < 0.1) pre-edge peaks [43,52,53].

Please cite this article in press as: M.-Y. Lee, et al., The targeted synthesis of single site vanadyl species on the surface and in the framework of silicate building block materials, Catal. Today (2010), doi:10.1016/j.cattod.2010.06.029

Table 3
Vanadium *K*-edge XANES features (referenced to vanadium foil (5465 eV))[a].

Entry	Sample description	Pre-edge shoulder (eV)	Pre-edge peak energy/$\Delta E_{½}$ (eV)	Pre-edge peak height	Main edge (eV)	Refs.
3C-vanadyl samples[b]						
1	Si_8Sn_8[c] + $VOCl_3$ (**1**)	4.3	6.12/2.3	0.80	17.4	This work
2	**1** + $SiCl_4$	4.3	6.15/2.5	0.80	17.0	This work
3	$Si_8Sn_8/VOCl_3 + Me_2SiCl_2$ followed by excess TMSCl	4.4	6.4/2.9	0.73	17.0	This work
1C-vanadyl samples[d]						
4	$SiCl_4$ platform + $VOCl_3$	4.0	6/2.8	0.80	17.0	This work
5	Me_2SiCl_2 platform + $VOCl_3$	4.1	6.1/2.9	0.86	17.0	This work
6	$Si_8O_{12}(OVOCl_x)_8$[e]	4.0	6/2.9	0.80	17.0	This work
7	~10% V_2O_5/SiO_2 hydrated	no[f]	6.0	0.56	16.7	[54]
8	~10% V_2O_5/SiO_2 dehydrated	nr[f]	6.0	0.76	18.9	[54]
9	$VOCl_3$/silica-100[g]	2.3	4.8	0.66	18.4	[8]
10	$VOCl_3$/silica-500[g]	2.4	4.9	0.67	18.3	[8]

[a] Values in table are eV above (higher energy) the vanadium foil reference edge position.
[b] 3-Connected vanadyl samples prepared as described in text. Entries 2 and 3 refer to samples exposed to second cross-linking dose (either $SiCl_4$ or Me_2SiCl_2) and a TMSCl dose to remove residual $SnMe_3$ groups.
[c] $Si_8Sn_8 = Si_8O_{12}(OSnMe_3)_8$.
[d] 1-Connected vanadyl samples prepared as described in text. An initial Si_8O_{12} platform is prepared via silane cross-linking followed by exposure to $VOCl_3$.
[e] Sample prepared by adding $Si_8O_{12}(OSnMe_3)_8$ to solution of excess $VOCl_3$ in CH_2Cl_2. Gravimetric analysis indicated that ~90% of the vanadyl groups in the sample were 1-connected.
[f] No, not observed; nr, not reported.
[g] Silica 100, 500 – aerosil silica dehydrated at 100 and 500 °C under vacuum. Samples contain 1C-vanadyl species, exclusively.

In the case at hand, we expect pseudo tetrahedral symmetry around vanadium as chloride ligands are exchanged for oxygen in these matrices. Therefore inversion symmetry should not be present and an intense 1s → 3d pre-edge transition is expected. Table 3 summarizes the peak heights for a number of the samples that have been prepared in this study relative to the absorption edge for vanadium metal (5465 eV). The pre-edge peaks all have intensities >0.7 consistent with the expected pseudo tetrahedral coordination geometry around vanadium. Examples of both 1-connected ($Cl_3VO(O–Si\equiv)$) and 3-connected ($OV(O–Si)_3$) have been described in the literature and are included in the table (entries 7–10) [8,54]. Our data closely match what has been presented in these previous studies.

A small shoulder is also observed on the pre-edge peaks recorded for all samples that we have prepared. While this shoulder has been observed before [8,36] in samples prepared by grafting vanadyl species to the surfaces of silica, there has been very little discussion of it in the literature. These previous studies do show that observation of this feature depends on the state of hydration of the surface. Pre-edge peaks for samples that contain significant amounts of physisorbed water or are exposed to water after grafting do not show a shoulder [8,36]. The observation of the shoulder here is consistent with the absence of water in both the synthesis and preparation of XAS samples prior to collection of X-ray data.

A second feature in the XANES region is observed when chloride is present in the first coordination sphere around vanadium. The lower half of ionization edge for 1- and 2-connected vanadyl sites exhibits a pronounced shoulder that is not present in the 3-connected sample (Fig. 2). This feature has been previously assigned to a vanadium based 1s → 4p simultaneous with ligand-to-metal shakedown transition [8,55,56]. The prominence/integrated intensity of this shoulder relative to the normalized edge increases with the number of chlorides bound to vanadium [56]. The presence of this feature qualitatively indicates whether chloride is bound to vanadium in these samples after the first and subsequent cross-linking reactions used to form the final matrices.

The main edge energies for the vanadyl sites in these samples are also summarized in Table 3. Very little variation in edge energy is observed throughout the entire matrix of sites and stages of cross-linking encompassed in this study. The energy of the edge is consistent with a +5 oxidation state for vanadium.

Taken together, the features observed in XANES region of these XAS spectra are quite rich in information about the vanadium sites in these matrices. Edge positions, pre-edge energies and peak heights are all consistent with the presence of non-centrosymmetric vanadyl +5 sites in the samples prepared here. The presence of a 1s → 4p shakedown transition, observed as a shoulder on the main ionization edge, signals the presence of chloride in the first coordination sphere of vanadium [8,36,52,55,57].

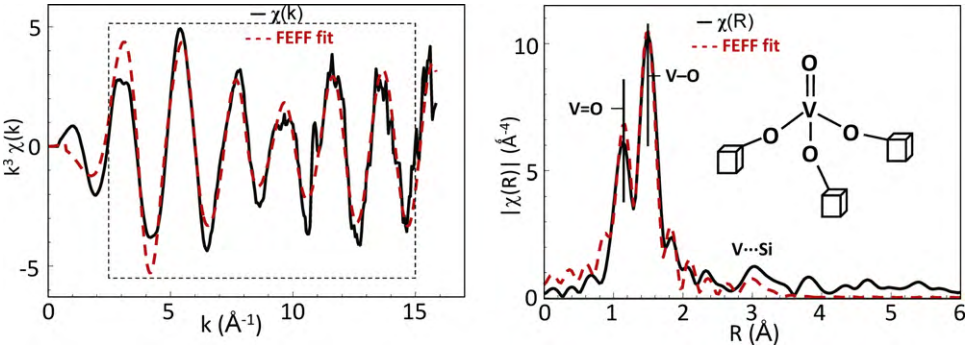

Fig. 3. 3C-vanadyl EXAFS *k*- and *R*-space plots. Dashed box shows the *k* range used in fits to structural models.

Please cite this article in press as: M.-Y. Lee, et al., The targeted synthesis of single site vanadyl species on the surface and in the framework of silicate building block materials, Catal. Today (2010), doi:10.1016/j.cattod.2010.06.029

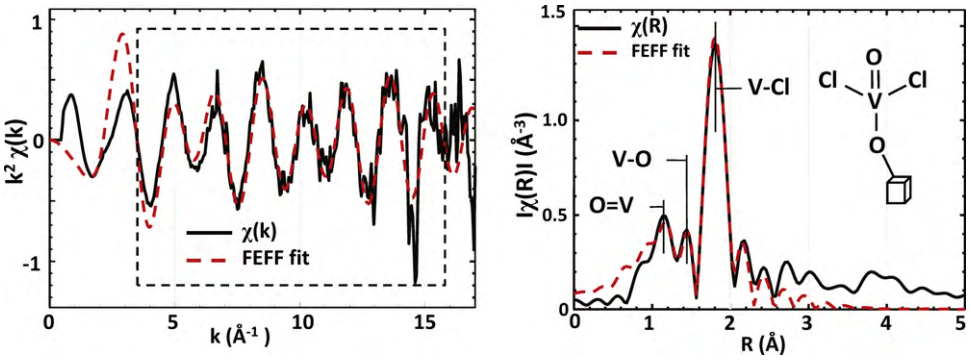

Fig. 4. 1C-vanadyl EXAFS *k*- and *R*-space plots. Dashed box shows the *k* range used in fits to structural models.

3.1.2. EXAFS analysis

Standard procedures (see Supplementary material) were used to extract backscattering fine structure in the EXAFS region from the smooth ionization edge background. *k*-Weighted EXAFS functions ($\chi(k)$) are presented in Figs. 3 and 4 for 1- and 3-connected vanadyl sites in the matrices. The first coordination sphere for vanadium in all of these samples is composed of one terminal vanadyl oxo ligand and a mix of oxygen and chloride ligands that depends on the connectivity achieved for vanadium at the time of synthesis. Embedded 3C-vanadyl sites will have three singly bound oxygens and no chlorides while EXAFS for the surface 1C-vanadyl sites should display components derived from two chlorides and one singly bound oxygen.

The EXAFS for the first coordination sphere of the intermediate, 2-connected vanadyl species (made from the mono isopropoxy complex ($O{=}VCl_2(OiPr)$) are indistinguishable from that observed for the 3-connected vanadyl. Essentially the same two backscattering shells (V=O and V–O) are observed in both cases. Furthermore, samples that contain mixtures of 1C-, 2C- and 3C-vanadyl sites exhibit EXAFS spectra in which the V=O, V–O and V–Cl distances are also indistinguishable within the experimental resolution and disorder (static and dynamic) limits. The only parameter that may be used to distinguish between single site samples and samples containing mixtures of vanadyl sites is the coordination number (CN) for each backscattering shell. Uncertainties in EXAFS derived CNs are frequently in the range of 20–30%. Therefore even when EXAFS data is used to define the first coordination sphere alone, it can still be quite challenging to use these data to determine site homogeneity with confidence.

The vanadyl group, common to all sites in this work, is expected to produce EXAFS single components at relatively short distances (1.5–1.6 Å) while features for the V–O and V–Cl ligands are expected at ~1.75 and ~2.15 Å, respectively. Fourier transforms of EXAFS data extracted from the smooth absorption edge (non-phase corrected *R*-space plots) for 1- and 3-connected vanadyl containing matrices illustrate the endpoints of the connectivity titration and clearly show all the features described above.

Table 4
Bond distances for vanadyl silanolates and chloro silanoates.

Compound (method)	V=O	V–O	V–Cl	Refs.
$VO(OSiPh_3)_3$ (XRD)	1.564	1.743 1.745		[61]
$[(c\text{-}C_6H_{11})_7Si_8O_{12})VO]_2$ (XRD)	1.564	1.772 1.737		[62]
$[VOCl(O_2Si^iBu_2)]_3$ (XRD)	1.589	1.727	2.1717	[60]
$VOCl_2(OCH_2CH_2OPh)$ (XRD)	1.5703	1.7134	2.1570 2.1715	[58]
$VO[OSi(O^tBu)_3]_3$ (EXAFS)	1.596	1.77		[59]

Structural models for the 1- and 3-connected vanadyl sites were developed from models based on examples in the literature (Table 4) [58–62]. Theoretical phase and amplitude functions for single scattering paths derived from FEFF multiple scattering theory were used to model EXAFS data for each sample. Figs. 3 and 4 display both $\chi(k)$ data and *R*-space plots overlaid with fits. Table 5 summarizes the final structural parameters obtained from the fits.

The correspondence between the theoretical phase and amplitude functions and experimental EXAFS supports the validity of the proposed structural models for both surface and embedded vanadyl samples. The bond distances obtained in this study are also consistent with corresponding data reported in the literature (Table 4). The refined coordination numbers for the two shells of singly bonded oxygen and chloride are consistent with gravimetric and solid state ^{51}V NMR data.

A detailed XAS study for a 1C-surface vanadyl species analogous to the one described here has been reported by Deguns et al. [8]. While the results reported here are in good agreement with this previous work, the authors concluded from a careful analysis of their data that the two chlorides bound to vanadium were inequivalent. We have subjected our data to a similar statistical analysis where models involving one or two distinct chlorides are present and have concluded that a two-chloride model is not justified for

Table 5
Structural parameters obtained from fits to EXAFS data[a].

	3C-vanadyl				1C-vanadyl			
	V=O	V–O	V–Cl	V···Si	V=O	V–O	V–Cl	V···Si
R (Å)	1.61	1.79	–	3.37	1.58	1.78	2.16	–
σ^2 (Å²)	0.001	0.002	–	0.01	0.0004	0.001	0.003	–
E_o (eV)	1.99	1.99	–	10.4	9.8	9.8	−1.6	–
CN	1 (set)	3 ± 0.1	–	CN (O)	1 (set)	1 (set)	2 (set)	–

[a] Additional fitting parameters as follows: amplitude reduction factor (S_0^2) 0.89 (3C-sample); 0.93 (1C-sample). Estimated uncertainties: backscattering shell distances: 0.2 Å; Debey Waller factors: 20%; E_o: 20%. Fit figures of merit: 3C-vanadyl: reduced χ^2 85; *R*-factor 6.3% (*R* range 1.2–4). 1C-vanadyl: reduced χ^2 5; *R*-factor 1.6% (*R* range 1.2–3).

Please cite this article in press as: M.-Y. Lee, et al., The targeted synthesis of single site vanadyl species on the surface and in the framework of silicate building block materials, Catal. Today (2010), doi:10.1016/j.cattod.2010.06.029

the samples described here. The precise reasons for this difference are at present unknown but two factors may be at play. First the single attached surface species could be rotating around the V–O bond and causing the V···Si feature to be dynamically disordered in the room temperature data considered here and second, surface hydroxyl groups are necessary in the grafting reactions used by Deguns et al. in contrast to the complete absence of hydroxyl groups or any type of acidic protons in the samples reported here.

Attempts to model a second shell of silicon atoms for the samples described here met with varying success. In the case of the 3C-embedded vanadyl sample, a feature that may represent a second shell of nonbonded silicon atoms was observed in *R*-space plots and subsequently modeled as such, locking the coordination number to that of oxygen at 1.75 Å. The surface vanadyl species exhibited no such feature and attempts to include a shell of long range silicon backscatterers were not successful. It is possible that mobility around the single point of attachment to the surface in this case creates large dynamic disorder in this shell which makes it unobservable at room temperature. Variable temperature data might provide information about such behavior [63,64].

The combination of gravimetric, SSNMR and EXAFS data provide a clear picture for the vanadyl sites in these samples. Gravimetric data establishes the connectivity of the vanadium atom to the surrounding matrix and can be used to provide initial values for coordination numbers in models used to fit EXAFS data. EXAFS data provide structural information about the sites present in the sample when suitable models can be found and used to generate phase and amplitude functions needed to fit $\chi(k)$ data. However, as noted above, neither EXAFS nor gravimetric data are particularly good at distinguishing between samples that contain mixtures of structurally similar species that average to the same connectivity as a single site. Solid state NMR data is then critical in addressing this question. Unfortunately, many catalytically active metals either cannot be observed by NMR or are significantly more challenging to interpret than the ^{51}V data presented here. In other work in our laboratories we have frequently encountered this situation and sought to develop methods to address this issue. Besides the catalytically active metal itself, oxygen is the only constituent of the active site that will also be found in most transition metal catalysts on metal oxide supports. ^{17}O solid state NMR has been used quite successfully to characterize both pure and mixed metal oxide materials [65–69]. One of the first challenges one faces in contemplating ^{17}O SSNMR experiments is the low sensitivity associated with the natural abundance of this isotope (0.04 atm%). We therefore developed an efficient synthesis of the stannylated silicate cube in which the terminal oxygens are selectively enriched with ^{17}O (I = 5/2). These oxygen atoms eventually become the points of attachment between the active metals and the matrix of building blocks around them. Our goal in this effort was to ascertain that solid state ^{17}O NMR of enriched samples could be used to (1) detect the active sites in the matrix and (2) distinguish between different sites if more than one was present.

3.2. A Multinuclear study of ^{17}O enriched in silicate building block matrices containing vanadyl groups

An efficient synthesis of the $Si_8O_{12}(^*OSnMe_3)_8$ cube which was enriched (40 atm%) with ^{17}O only in the terminal oxygen positions is described in the experimental section. Two ^{17}O enriched-vanadyl samples were prepared. Following the procedure given in the experimental section, the first contained only 3C-vanadyl sites in the matrix based on gravimetric data. The second was prepared by reacting a limiting amount of enriched cube with $VOCl_3$ to produce a sample that had a mixture of predominantly 1-connected (surface) and 2-connected vanadyl sites throughout the matrix. Gravimetric analysis yielded an average connectivity of 1.4 for the vanadyl sites in the matrix and indicated that virtually all trimethyltin groups had been replaced with vanadyl species. This sample is hereafter referred to as the "high-V" sample.

^{29}Si SSNMR MAS and CP-MAS spectra (Supplementary material, Figs. S6 and S7) for these samples show two signals in the traditional silicate chemical shift region (−100 to −120 ppm). Deconvolution of the two overlapping signals observed in the case of the 3C sample gave rise to resonances at −102 ppm (major) and a second at −107 ppm (minor). Silicon bound to tin through oxygen gives rise to signals at −101 ppm [18,70]. Leading to the assignment of the resonance at −102.0 ppm to silicons bearing unreacted –OSnMe$_3$ groups and the −107.0 ppm resonance to silicons that are bound to vanadium through oxygen. Cross-polarization experiments are consistent with this assignment. The ratio of the areas of the two signals is estimated to be 2:1, respectively. Gravimetric data for this sample indicates that all vanadyl sites are connected to three Si_8O_{20} cubes which leads a ratio of unreacted cube corners to vanadium linked corners of 5:3. These two values are in reasonable correspondence with one another considering that the relative relaxation rates of the two types of silicon involved could be different and affect the relative peak integrations.

The high-V sample shows a single, asymmetric ^{29}Si SSNMR peak at −108 ppm consistent with the preceding assignment to Si–O–V groups in the sample. Gravimetric analysis of this sample gives rise to a connectivity of 1.4 indicating that both 1C- and 2C-vanadyl centers are present in the sample. Deconvolution of this peak into two signals corresponding to silicons bound to either 1C- or 2C-vanadyl groups was attempted making the following assumptions: First, no other signals were present. Second, from previous studies on similar building block matrices, a good measure for the line widths typically observed for cube silicons (reflecting the chemical dispersion of the amorphous matrix) is estimated to be ∼350 Hz. With these two assumptions the line shape was well simulated by a mixture of two signals with chemical shift values of −105.3 and −108.4 ppm and in a 1:2 ratio. These signals are assigned to 2C- and 1C-vanadyl bearing cube corners, resp. The ratio of these two types of silicon atoms derived from ^{29}Si NMR agrees well with gravimetric data. Finally cross-polarization experiments (Supplementary material) caused all silicon signals to be significantly reduced in intensity consistent with the lack of nearby protons in the matrix and arguing against any silanol or residual Si–O–SnMe$_3$ groups in the matrix.

A ^{51}V SSNMR spectrum of this sample (Supplementary material) conclusively showed the presence of 1C- and 2C-vandyl groups in the matrix. The spinning sideband patterns for these two signals are much wider than the chemical shift difference of the isotropic peaks such that considerable overlap is observed. This high degree of overlap prevented an accurate determination of the relative amounts of the two vanadyl species present.

1D ^{17}O SSNMR spectra for both of these samples are presented in Fig. 5. The 3C-vanadyl sample shows a prominent signal with a peak envelop from 0 to −200 ppm and evidence for a much weaker signal centered roughly at 275 ppm. The high-V sample exhibits a similar pattern of two signals with their relative intensities reversed: a large signal centered around 300 ppm and a smaller signal at −50 ppm. Based on gravimetric data and the silicon SSNMR spectra we assign the ^{17}O peak at ∼275 ppm to oxygen atoms linking silicon and vanadium and the one centered roughly at −50 ppm to oxygen atoms linking silicon and tin. Correlations of ^{17}O isotropic chemical shifts in metal oxide matrices have been reported recently [65]. The coordination number for oxygen (terminal, μ, μ_2, . . ., μ_6), bond angles and ionicity of M–O–M bonds have both been identified as contributing significantly to ^{17}O isotropic shifts. Within the context of oxygen bridging two metals, the O–Sn bond is expected to be more covalent than either O–Si or O–V bonds thus leading to the expectation of higher shielding around oxygen and assignment

Please cite this article in press as: M.-Y. Lee, et al., The targeted synthesis of single site vanadyl species on the surface and in the framework of silicate building block materials, Catal. Today (2010), doi:10.1016/j.cattod.2010.06.029

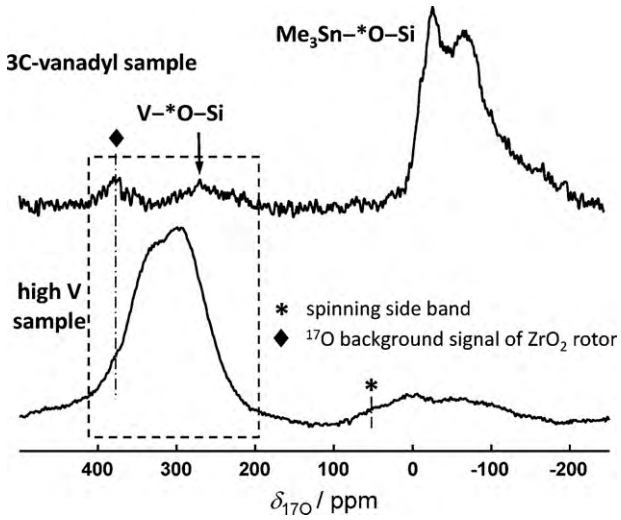

Fig. 5. 1D ^{17}O MAS SSNMR of ^{17}O enriched 3C-vanadyl and high-V samples.

to the signal observed at ∼−50 ppm in the spectra described above. The signal observed in the region around 300 ppm is then assigned to V–O–Si links in these spectra.

The interpretation of quadrupolar NMR line shapes requires a detailed knowledge of several factors including nuclear spin, quadrupolar coupling constant, electric field gradient and asymmetry around the spin active nucleus [65]. In many cases 1D spectra do not contain enough information to deconvolute the effects of these factors together with dipolar coupling and chemical shift anisotropy on observed line shapes. Two dimensional, multiple quantum magic angle spinning (MQMAS) techniques have revolutionized many areas of NMR spectroscopy [71]. In the case of quadrupolar nuclei, MQMAS techniques can be used to separate out the isotropic shift from other factors that influence peak positions and line shape. Triple quantum MQMAS data were collected for both the 3C and high-V samples above. The full 2D-spectrum for the 3C-vanadyl sample is presented in Fig. 6 along with 1D spectral slices as indicated. Isotropic shift data can be obtained from the δ_{F2} axis of the MQMAS spectrum and the results of preliminary line shape analyses are shown in the figure.

The MQMAS spectrum for the 3C-vanadyl sample shows a prominent set of signals in the region between 50 and −75 ppm which has been assigned to Sn–O*–Si links to unreacted $Me_3Sn–O–Si_{cube}$ groups in the sample. A second small feature assigned to V–O*–Si groups is observed in the region between 200 and 250 ppm but the signal to noise ratio for this signal in the MQMAS spectrum is very low. Preliminary quadrupole line shape analyses have been performed for both signals. In the case of the Sn–O–Si signal, the isotropic axis of the 2D spectrum indicates that two different groups are present and the overall signal has been modeled as the sum of two spectroscopically distinct ^{17}O sites as shown in the figure. The 1D spectrum indicates that the envelope for this signal is much broader than what is observed in the MQMAS spectrum. The signal to noise and lack of singularities in the MQMAS data make an accurate determination of the isotropic shift difficult at this time but we estimate it to be below 300 ppm.

Fig. 7 presents only the downfield region of a MQMAS spectrum for the high-V sample. The ^{17}O signal in the Si–O*–Sn region (50 to −50 ppm) is quite small and overlapped with a spinning side band from the major V–O*–Si signal thus preventing detailed analysis. The projection of the signal shown in Fig. 7 along the F2 axis may be described as a pseudo Gaussian that shows little if any structure relating to the quadrupole line shape expected for these 2-coordinate, bridging oxygens. The projection along the isotropic axis (F1) is similar but the presence of two signals is indicated by the width and asymmetry of the envelop. Both ^{51}V and ^{29}Si spectra indicate that indeed 1C- and 2C-vanadyl sites are present in this sample and therefore the signal was fit to two Gaussian signals as indicated in the figure. Slices along F2 at the positions of these two signals are shown in the figure. Very little quadrupole "structure" can be seen in either signal and therefore independent determinations of the quadrupole parameters and the isotropic shift associated with these signals cannot be made at this time. The reason for this is most probably significant chemical shift dispersion that results from the amorphous nature of these glasses [68]. The fits to observed line shapes shown in Fig. 7 are based upon initial values of the quadrupolar parameters for similar metal-silicate systems in the literature [65,66]. Final fit parameters are summarized in Supplementary material (Table S1). From this analysis, isotropic chemical shifts of the two V–O*–Si signals in Fig. 7 are estimated to be above 300 ppm which is distinct from that observed in the spectra for the enriched 3C-vanadyl sample.

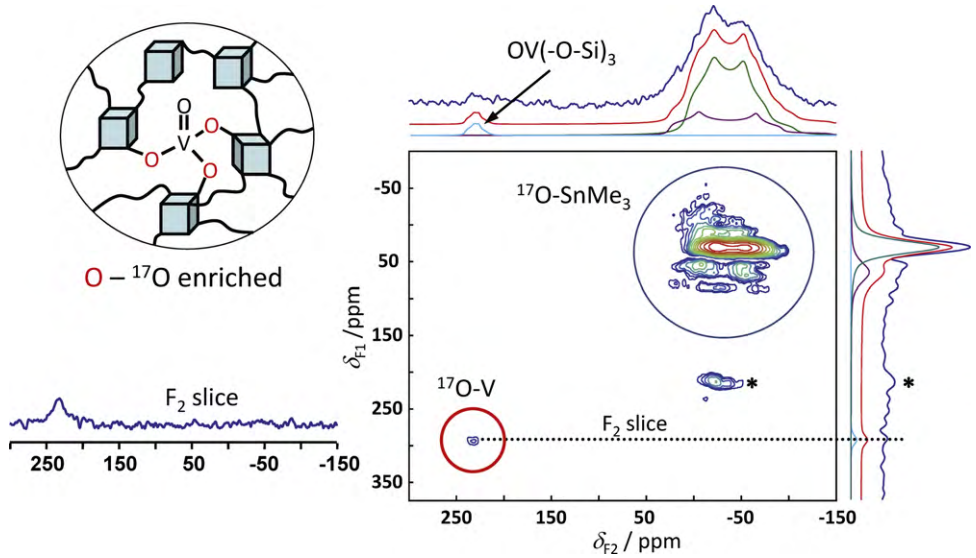

Fig. 6. Sheared *z*-filter ^{17}O MQMAS NMR spectrum of "3C-vanadyl" Si_8O_{12} material recorded using ϕ_1 (hard pulse) of 3.3 μs, ϕ_2 (soft pulse) of 1.1 μs and ϕ_3 of 10 μs at rotation rate of 14 kHz. The isotropic and anisotropic dimensions are along δ_{F1} (vertical) and δ_{F2} (horizontal) axis, respectively. * Denotes spinning sideband.

Please cite this article in press as: M.-Y. Lee, et al., The targeted synthesis of single site vanadyl species on the surface and in the framework of silicate building block materials, Catal. Today (2010), doi:10.1016/j.cattod.2010.06.029

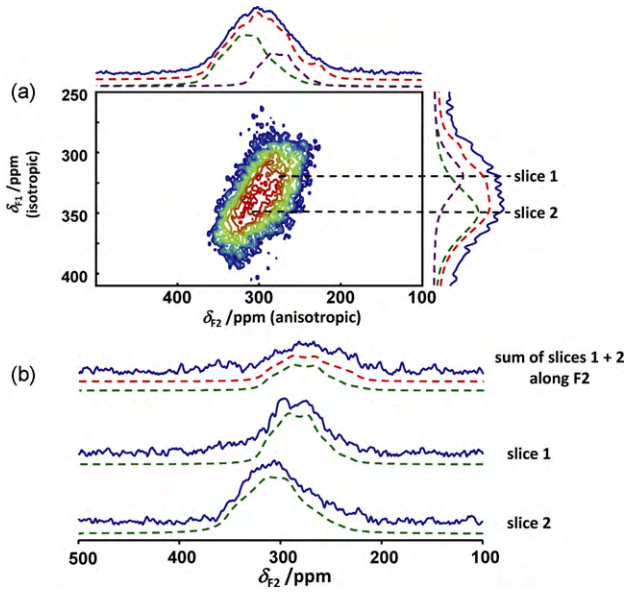

Fig. 7. Sheared z-filter ^{17}O MQMAS NMR spectrum of "high-V" Si_8O_{12} material: (a) recorded using ϕ_1 (hard pulse) of 3.3 μs, ϕ_2 (soft pulse) of 1.1 μs and ϕ_3 of 10 μs at rotation rate of 14 kHz. The isotropic and anisotropic dimensions are along δ_{F1} (vertical) and δ_{F2} (horizontal) axis, respectively. (b) Two oxygen resonances ^{17}O quadrupole resonances along slices 1 and 2 on F2 axis.

The main focus of the work described here is to ascertain whether ^{17}O SSNMR can be used to detect and identify the vanadyl sites are present in these matrices. We have been partially successful in this endeavor. In the two ^{17}O enriched samples that were prepared and analyzed here we have been able to correlate ^{29}Si, ^{51}V and ^{17}O SSNMR data to reach the following conclusions: (1) ^{17}O SSNMR (1D and MQMAS) can be used to detect the vanadyl sites in Si_8O_{12} matrices that are selectively enriched (40 atm%) at catalytically relevant metal loadings; (2) ^{17}O isotropic shifts are sensitive to remote changes at the vanadium center (changing numbers of chloride ligands) which can be used to identify specific sites in these matrices; and (3) The relative ratio of sites in the high-V sample, estimated from gravimetric analysis and ^{29}Si SSNMR data is 2:1 (1C-:2C).

4. Conclusions

A simple strategy by which silicate matrices containing atomically dispersed vanadyl groups is demonstrated. Using a combination of build block techniques to maintain site isolation, and a sequential addition strategy to control the connectivity of the vanadyl group to the surrounding building blocks, silicate matrices containing only 1-connected, 2-connected or 3-connected vanadyl centers have been prepared. These matrices have been characterized by a series of physical and spectroscopic techniques that together uniquely define both the identify and distribution of vanadium based sites in the matrix. Gravimetric measurements indirectly establish the average connectivity achieved at vanadium as it assumes cross-linking positions between Si_8O_{20} cubes. The ^{51}V isotropic chemical shift is sensitive to the number and type of ligands around the vanadyl group and can therefore be used to distinguish the different sites contributing to average connectivities derived from gravimetric data. X-ray absorption data can be used to fingerprint the vanadyl sites present (e.g. chloride feature in XANES) as well as provide structural data (EXAFS models) for the sites present in the matrix. However, if any one of these three types of data is missing, defining the number and types of sites present in these matrices becomes much more difficult and less accurate. For this reason, a general method to incorporate a second spectroscopic probe into the matrix was developed. Selective ^{17}O enrichment of the silicate building block at the oxygen atoms bound to vanadium was accomplished and both 1D and 2D (MQMAS) spectra recorded. A preliminary analysis of the isotropic ^{17}O SSNMR signals observed for a single site sample as well as one with a mixture of vanadyl sites illustrate the potential of ^{17}O NMR to independently identify and quantify the types of vanadyl sites present in these matrices.

The synthetic methodology illustrated here in the case of vanadyl chloride can be applied quite broadly to many high valent metals and main group elements as cross-linking precursors. Equally important is the strategy presented here for identifying and following changes that occur in the catalyst ensemble at each stage of synthesis. Current investigations are focused in two directions. First, analogous single site catalysts based on other metals (Ti, W, Sn, Al, and Ga) are being developed and characterized as above. Second, a correlation between site identity and the activity is being developed for a number of solid acid and oxidation reactions for these single site catalysts.

Acknowledgments

The authors thank Drs. Syed Khalid and Anatoly Frenkel of the National Synchrotron Light Source (NSLS) at Brookhaven National Laboratory for helpful discussions. We are grateful to the US Department of Energy (DE-FG02-01ER15259) for the financial support of this project.

Appendix A. Supplementary data

Supplementary data associated with this article can be found, in the online version, at doi:10.1016/j.cattod.2010.06.029.

References

[1] J.M. Thomas, R. Raja, D.W. Lewis, Angew. Chem. Int. Ed. Engl. 44 (2005) 6456–6482.
[2] P. Zhu, M.E.v.d. Boom, H. Kang, G. Evmenenko, P. Dutta, T.J. Marks, Chem. Mater. 14 (2002) 4982–4989.
[3] G. Busca, Chem. Rev. 107 (2007) 5366–5410.
[4] J. Macht, R.T. Carr, E. Iglesia, J. Catal. 264 (2009) 54–66.
[5] S.T. Oyama, Res. Chem. Intermed. 15 (1991) 165–182.
[6] S.V. Ley, I.R. Baxendale, in: D.C. Sherrington, A.P. Kybett (Eds.), Supported Catalysts and Their Applications, vol. 266, Royal Society of Chemistry, Cambridge, 2001, p. 270.
[7] G. Mul, J.A. Moulijn, in: J.A. Anderson, M.F. García (Eds.), Supported Metals in Catalysis, vol. 5, Imperial College Press, 2005, pp. 1–31.
[8] E.W. Deguns, Z. Taha, G.D. Meitzner, S.L. Scott, J. Phys. Chem. B 109 (2005) 5005–5011.
[9] S.L. Scott, J.M. Basset, J. Mol. Catal. 86 (1994) 5–22.
[10] K. Inumaru, T. Okuhara, M. Misono, J. Phys. Chem. 95 (1991) 4826–4832.
[11] C. Coperet, M. Chabanas, R.P. Saint-Arroman, J.M. Basset, Angew. Chem. Int. Ed. 42 (2003) 156–181.
[12] M.M. Branda, R.A. Montani, N.J. Castellani, Surf. Sci. 446 (2000) L89–L94.
[13] E.W. Bittner, B.C. Bockrath, J.M. Solar, J. Catal. 149 (1994) 206–210.
[14] W.F. Krupke, IEEE J. Sel. Top. Quantum. Electron. 6 (2000) 1287–1296.
[15] S. Dai, M.C. Burleigh, Y.H. Ju, H.J. Gao, J.S. Lin, S. Pennycook, C.E. Barnes, Z.L. Xue, J. Am. Chem. Soc. 122 (2000) 992–993.
[16] G. Wulff, Angew. Chem. Int. Ed. Engl. 34 (1995) 1812.
[17] Y.E. Seidel, A. Schneider, Z. Jusys, B. Wickman, B. Kasemob, R.J. Behm, Faraday Discuss. 140 (2008) 167–184.
[18] J.C. Clark, C.E. Barnes, Chem. Mater. 19 (2007) 3212–3218.
[19] I.E. Wachs, G. Deo, M.V. Juskelis, B.M. Weckhuysen, Stud. Surf. Sci. Catal. 109 (1997) 305–314.
[20] R. Rulkens, J.L. Male, K.W. Terry, B. Olthof, A. Khodakov, A.T. Bell, E. Iglesia, T.D. Tilley, Chem. Mater. 11 (1999) 2966–2973.
[21] R. Rulkens, T.D. Tilley, J. Am. Chem. Soc. 120 (1998) 9959–9960.
[22] B.M. Weckhuysen, D.E. Keller, Catal. Today 78 (2003) 25–46.
[23] N. Magg, B. Immaraporn, J.B. Giorgi, T. Schroeder, M. Bäumer, J. Döbler, Z. Wu, E. Kondratenko, M. Cherian, M. Baerns, P.C. Stair, J. Sauer, H.-J. Freund, J. Catal. 226 (2004) 88–100.
[24] H. Tian, E.I. Ross, I.E. Wachs, J. Phys. Chem. B 110 (2006) 9593–9600.
[25] N.N. Ghosh, J.C. Clark, G.T. Eldridge, C.E. Barnes, Chem. Commun. (2004) 856–857.
[26] M. Newville, J. Synchrotron. Rad. 8 (2001) 322–324.

[27] S.I. Zabinsky, J.J. Rehr, A. Ankudinov, R.C. Albers, M.J. Eller, J. Phys. Rev. B (1995) 2995.
[28] F.J. Feher, K.J. Weller, Inorg. Chem. 30 (1991) 880–882.
[29] F.J. Feher, K.J. Weller, Chem. Mater. 6 (1994) 7–9.
[30] P.H. Mutin, A. Vioux, Chem. Mater. 21 (2009) 582–596.
[31] B. Alonso, C. Sanchez, J. Mater. Chem. 10 (2000) 377–386.
[32] M.A. Banares, M. Martinez-Huerta, X. Gao, I.E. Wachs, J.L.G. Fierro, Stud. Surf. Sci. Catal. 130D (2000) 3125–3130.
[33] M.A. Banares, M.V. Martinez-Huerta, X. Gao, J.L.G. Fierro, I.E. Wachs, Catal. Today 61 (2000) 295–301.
[34] L.J. Burcham, G. Deo, X. Gao, I.E. Wachs, Top. Catal. 11/12 (2000) 85–100.
[35] G. Deo, I.E. Wachs, J. Haber, Crit. Rev. Surf. Chem. 4 (1994) 141–187.
[36] X. Gao, S.R. Bare, B.M. Weckhuysen, I.E. Wachs, J. Phys. Chem. B 102 (1998) 10842–10852.
[37] J. Haber, P. Nowak, E.M. Serwicka, I.E. Wachs, Bull. Pol. Acad. Sci. Chem. 48 (2000) 337–346.
[38] K. Tran, M.A. Hanning-Lee, A. Biswas, A.E. Stiegman, G.W. Scott, J. Am. Chem. Soc. 117 (1995) 2618–2626.
[39] G.L. Rice, S.L. Scott, Langmuir 13 (1997) 1545–1551.
[40] F.J. Feher, R.L. Blanski, Organometallics 12 (1993) 958–963.
[41] O.B. Lapina, M.A. Mats'ko, T.B. Mikenas, V.A. Zakharov, E.A. Paukshtis, D.F. Khabibulin, A.P. Sobolev, Kinet. Catal. 42 (2001) 553–560.
[42] N. Das, H. Eckert, H. Hu, I.E. Wachs, J.F. Walzer, F.J. Feher, J. Phys. Chem. 97 (1993) 8240–8243.
[43] F. Farges, G.E. Brown, J.J. Rehr, Phys. Rev. B 56 (1997) 1809–1819.
[44] S.D. Kelly, K.M. Kemner, G.E. Fryxell, J. Liu, S.V. Mattigod, K.F. Ferris, J. Phys. Chem. B 105 (2001) 6337–6346.
[45] F. Farges, Phys. Rev. B (2005) 71.
[46] M. Newville, B. Ravel, D. Haskel, J.J. Rehr, E.A. Stern, Y. Yacoby, Phys. B: Condens. Matter B208&209 (1995) 154–155.
[47] L.A. Grunes, Phys. Rev. B. 27 (1983) 2111–2131.
[48] Z.Y. Wu, Phys. Rev. B 55 (1997) 10382–10391.
[49] A.L. Ankudinov, B. Ravel, J.J. Rehr, S.D. Conradson, Phys. Rev. B 58 (1998) 7565–7576.
[50] B. Ravel, J. Alloys Compd. 401 (2005) 118–126.
[51] J.J. Rehr, R.C. Albers, Rev. Mod. Phys. 72 (2000) 621–654.
[52] J. Wong, F.W. Lytle, R.P. Messmer, D.H. Maylotte, Phys. Rev. B 30 (1984) 5596.
[53] S. Bordiga, S. Coluccia, C. Lamberti, L. Marchese, A. Zecchina, F. Boscherini, F. Buffa, F. Genoni, G. Leofanti, G. Petrini, G. Vlaic, J. Phys. Chem. 98 (1994) 4125–4132.
[54] X. Gao, S.R. Bare, B.M. Wechhuysen, I.E. Wachs, J. Phys. Chem. B 102 (1998) 10842–10852.
[55] R.A. Bair, W.A. Goddard, Phys. Rev. B 22 (1980) 2767–2776.
[56] K.S. Finnie, V. Luca, P.D. Moran, J.R. Bartlett, J.L. Woolfrey, J. Mater. Chem. (2000) 10.
[57] S. Yoshida, T. Tanaka, T. Hanada, T. Hiraiwa, H. Kanai, T. Funabiki, Catal. Lett. 12 (1992) 277–286.
[58] E.C.E. Rosenthall, F.Z. Girgsdies, Z. Anorg. Allg. Chem 628 (2002) 1917.
[59] R. Rulkins, J.L. Male, K.W. Terry, B. Olthof, A. Khodakov, A.T. Bell, E. Igleisa, T.D. Tilley, Chem. Mater. 11 (1999) 2966–2973.
[60] H.-J. Gosink, H.W. Roesky, M. Noltemeyer, H.-G. Schmidt, C. Freier-Erdmegger, G.M. Scheldriek, Chem. Ber. (1993) 126.
[61] H. Huang, C.W. DeKock, Inorg. Chem. 32 (1993) 2287–2291.
[62] F.J. Feher, J.F. Walzer, Inorg. Chem. 30 (1991) 1689–1694.
[63] C.E. Barnes, Y. Shin, S. Saengkerdsub, S. Dai, Inorg. Chem. 39 (2000) 862.
[64] G. Meitzner, J. Gardea-Torresdey, J. Parsonsb, S.L. Scott, E.W. Deguns, Microchem. J. 81 (2005) 61–68.
[65] S.E. Ashbrook, M.E. Smith, Chem. Soc. Rev. 35 (2006) 718–735.
[66] F. Babonneau, C. Bonhomme, C. Gervais, J. Maquet, J. Sol–Gel Sci. Technol. 31 (2004) 9–17.
[67] T.J. Bastow, P.J. Dirken, M.E. Smith, H.J. Whitfield, J. Phys. Chem. 100 (1996) 18539–18545.
[68] J.F. Stebbins, J.V. Oglesby, S.K. Lee, Chem. Geol. 174 (2001) 63–75.
[69] K.T. Mueller, Y. Wu, B.F. Chmelka, J. Stebbins, A. Pines, J. Am. Chem. Soc. 113 (1991) 32–38.
[70] J.C. Clark, S. Saengkerdsub, G.T. Eldridge, C. Campana, C.E. Barnes, J. Organomet. Chem. 691 (2006) 3213–3222.
[71] A. Medek, L. Frydman, J. Braz. Chem. Soc. 10 (1999) 263–277.

Please cite this article in press as: M.-Y. Lee, et al., The targeted synthesis of single site vanadyl species on the surface and in the framework of silicate building block materials, Catal. Today (2010), doi:10.1016/j.cattod.2010.06.029